Algerian Journal of Biosciences
ISSN: 2716-9375
Journal homepage:
https://www.journal.acse.science/index.php/ajb/index

Original Article

Synthesis of silver nanoparticles using *Solanum tuberosum* peels' extract and their activity against multi drug resistant bacteria

Kerai Dhrutiben[a], Betty Mbatia [a]*, and Naumih Noah[a]

[a] *School of Pharmacy and Health Sciences, United States International University (USIU-A), Nairobi, Kenya*

ARTICLE INFOR

Article history:
Received 08 July 2023
Revised 27 November 2023
Accepted 18 December 2023

Keywords:
Antimicrobial resistance;
Nanotechnology;
Biogenic;
Silver nanoparticules ;
MRSA;
E. coli.

ABSTRACT

Antimicrobial resistance is a global health concern. Nanoparticles are increasingly being used as an alternative to overcome microbial drug resistance. The synthesis of nanoparticles from crop residuals has the dual potential of combating antimicrobial resistance and addressing waste disposal challenges. In this study ethanolic extract from *Solanum tuberosum* peel varieties were investigated for the synthesis of silver nanoparticles (AgNPs) and their activity against methicillin-resistant *Staphylococcus aureus* and multidrug-resistant *Escherichia coli* evaluated. The formation of the AgNPs was confirmed using UV-Vis spectroscopy and Fourier Transform Infra-Red (FTIR) analysis, while size was confirmed using dynamic light scattering (DLS). Disc diffusion method was used to evaluate antimicrobial activity. Russet brown and red bliss potato peel varieties showed positive results for the presence of alkaloids, polyphenols, and flavonoids. UV-Vis spectroscopy of synthesized AgNPs showed prominent peaks at 435 and 430nm, while DLS showed a size of 391.5 and 203.00 nm for russet brown and red bliss, respectively. FTIR analysis for the crude extracts and nanoparticles showed a change in peaks, confirming that bio-reduction took place. Major peaks for brown russet nanoparticles were observed at 3337 cm^{-1}, 1634 cm^{-1},1055 $cm^{-1,}$ while major peaks for red bliss nanoparticles were observed at 3330 cm^{-1}, 1634 cm^{-1}, and 1054 cm^{-1}. Brown russet nanoparticles showed better activity against *S. aureus,* while red bliss nanoparticles had better activity against *E. coli.* Nanoparticles synthesized from both varieties showed antimicrobial activity against gram-positive and gram-negative bacteria.

1. Introduction

Antimicrobial resistance occurs when microbes such as bacteria, fungi, parasites, and viruses gain a competitive advantage over current antimicrobial regimens. This provides them with a characteristic that makes them immune to antimicrobials, hence making treatment and control of diseases difficult. Antimicrobial resistance is one of the major global health threats that hinder the achievement of sustainable development goals [1]. Antimicrobial resistance occurs naturally through various mechanisms during replication via mutations that benefit the microbe. However, the process is accelerated by irrational drug use, especially of antibiotics [2]. Over the years, abuse of antibiotics has resulted in the development of strains that are multi-drug resistant [3]. Of the commonly known drug-resistant bacteria are *Escherichia coli* and *Staphylococcus aureus*. *S. aureus* gained resistance by alteration of the penicillin-binding protein giving rise to Methicillin-resistant *S. aureus* [4]. *E. coli* has emerged resistant to multiple major classes of antibiotics attributed to multiple beta-lactamase enzymes and horizontal gene transfers via plasmids [5].

In order to combat antimicrobial resistance, nanotechnology, an advancing technology involving nanoparticles, has been exploited. Nanotechnology involves the modification and utilization of both inorganic and organic ions at the nanoscale from a size range of 1nm - 100nm [6]. Nanoparticles elicit their action via multiple simultaneous steps which makes it difficult for bacterial cells to become resistant to nanoparticles [7]. For a bacterial species to become resistant, it will have to evolve with multiple gene mutations that can evade the multiple antibacterial effects of nanoparticles. Nanoparticles cause mechanical damage to the cell via reactive oxygen species production, electrostatic neutralization, and interaction

* Corresponding author :Betty N. Mbatia . *Tel.: +254730116721*
E-mail address: bembatia@usiu.ac.ke
Peer review under responsibility of University of El Oued.2023
DOI : https://doi.org/10.57056/ajb.v4i2.146

with the bacterial DNA and proteins which eventually have a bactericidal effect [8].

Silver nanoparticles (AgNPs) are one of the metallic nanoparticles with proven antibacterial properties. They are reported to have a broad spectrum of activity with multiple mechanisms [7]. Silver ions have a positive charge which exhibits interaction with proteins and negatively charged DNA which disrupts protein synthesis. Silver nanoparticles have a positive charge which can neutralize bacterial cell membrane and eventually lead to bactericidal effects by altering its permeability [9].

Chemical or physical processes are used in traditional nanoparticle synthesis, both of which have significant limitations. Physical methods require very high temperatures and result in low yields [10]. Chemical methods require costly equipment, and utilize either toxic chemicals or release toxic by-products which are hazardous to the environment [10]. Biogenic synthesis using natural resources such as microorganisms or plants to synthesize nanoparticles presents an alternative to these drawbacks. It utilizes a low amount of energy, results in minimum environmental harm, and is cost-effective [11]. Biogenic synthesis of nanoparticles involves the reduction of metal ions using plant phytochemicals such as polyphenols, alkaloids, terpenoids, and sugars to synthesize metal nanoparticles [12]. The annual production of potatoes in Kenya are up to 3 million metric ton [13]. However, the potato peel waste which constitutes 6-10% of potato processing remains underutilized, presenting a management and environmental concern, therefore, a greater need to maximize their potential benefit [14].

Solanum tuberosum, commonly referred to as Irish potato can be an economical, safe, and convenient choice for nanoparticle synthesis. Irish potato peels have reported antimicrobial activity against bacterial species such as *S. aureus* and *P. aeruginosa* [15]. Potato peels are a rich source of alkaloids and polyphenols which act as stabilizing and reducing agents for nanoparticle synthesis [16]. The potato peels have a higher content of polyphenols than the flesh of the potato [17]. Some of the abundant polyphenols include caffeic acid, chlorogenic acid, protocatechuic acid, and gallic acid [18].

The aim of the study was to investigate the potential of varieties of *S. tuberosum* peel extracts for the biogenic synthesis of silver nanoparticles with antimicrobial activity against *E. coli* and *S. aureus* strains.

2. Materials and Methods

2.1 Sample collection

Two varieties of *S. tuberosum* i.e., the brown russet potato and red bliss potato were procured from Ngara city market, Nairobi (Latitude -1.274665 & longitude 36.829065). Specimens of the russet brown and red bliss potato samples were deposited and identified by a botanist and taxonomist, at the USIU-Africa School of Pharmacy and Health Sciences herbarium.

2.2 Preparation of Solanum Tuberosum aqueous extract

The method described was used with some modifications [19]. Briefly, the potatoes were washed with water, dried, and peeled using a mechanical peeler. The peels were collected and oven-dried at 45ºC. The dry matter content was determined as follows:

$$\frac{Weight\ of\ dry\ peel}{Weight\ of\ wet\ peel} \times 100$$

The peels were then ground to form a fine powder. Powder weighing 400g was macerated for 72 hours using 400ml of 100% ethanol. The extract was filtered using a Buchner funnel followed by evaporation at 40ºC in a rotatory evaporator. The dry extract was stored at 4 ºC [20].

2.3 Phytochemical characterization

The method described was used to test for phenols [21]. Dry potato peel extract weighing 0.05g was dissolved in 6ml of distilled water. Two ml of the potato peel extract was added with three drops of 1% $FeCl_3$ into a test tube for each extract. The formation of a dark, green, black colour indicated the presence of phenols. The alkali reagent method described was used to test for flavonoids [21]. Two ml of each potato extract was added to the test tube followed by the addition of three drops of dilute NaOH. The formation of yellow orange colour indicated the presence of flavonoids. To determine the presence of alkaloids, the method described was used [22]. Two ml of each extract was added to the test tube followed by the addition of three drops of picric acid. A yellow crystalline precipitate formation indicated the presence of alkaloids.

2.4 Silver nanoparticle synthesis

Analytical grade (99.7%) silver nitrate (0.1699g) from Sigma Aldrich was used to prepare a 1mM silver nitrate solution [6]. Aqueous Silver nitrate solution (50 ml, 1mM) was added to a 500ml Erlenmeyer flask. Dry potato peel extract weighing 0.05g of each variety was dissolved in 5 ml of distilled water and filtered. The acidic pH was adjusted to 8 using NaOH as this had been previously determined as the optimum pH for the synthesis of AgNPs using sweet potatoes [23]. The extract was then added dropwise into the 1mM $AgNO_3$ solution with continuous stirring and at a temperature of 70°C. These had been previously determined as optimal temperatures for $AgNO_3$ from jackfruit peels in our labs. The gradual colour change was monitored at regular intervals. The presence of silver nanoparticles was confirmed using UV-Vis spectrophotometry (Cary60, Agilent) using a wavelength ranging from 190-800nm. An absorption peak between the range of 400-450nm indicated the presence of metallic silver nanoparticles [24].

2.5 Optimization of potato peel extract concentration for the synthesis of nanoparticles

Dry potato peel extract weighing 0.05g, 0.1g, and 0.2g of each variety was dissolved in 5ml of distilled water and filtered. The potato peels solutions were then added to 500 ml flasks containing 50 ml of 1mM silver nitrate solution. Formation of the nanoparticles was initiated as described previously.

2.6 FTIR analysis

FTIR analysis (FT/IR-4700, Jasco Corporation) was done for the *S. tuberosum* peel extract and the silver nanoparticles synthesized from each of the varieties. The characterization was performed in the range of 4000-500cm^{-1} at room temperature [23].

2.7 Zeta potential and dynamic light scattering

The Zeta size method was used to determine the zeta potential of the nanoparticles while the dynamic light scattering method was used to determine the average particle size. Analysis was done using Zetasizer Nano ZS, Malvern Panalytical, Malvern U.K. The samples were analyzed using the method described [23].

2.8 Testing of antimicrobial activity

The disc diffusion agar method was used to determine the zones of inhibition [25]. Mueller Hinton (Oxoid) agar powder weighing 38g was suspended in a 1L flask with distilled water and mixed until it completely dissolved. The media and Petri dishes were sterilized by autoclaving at 121 ℃ for fifteen minutes. The liquid was allowed to cool to 45 ℃ before pouring into Petri dishes and allowed to solidify.

The strains used were Methicillin-resistant *S. aureus, S. aureus, E. coli,* and a multi-drug resistant strain of *E. coli*. Fresh cultures of the strains were swabbed and placed in a 5ml test tube with normal saline. The bacterial suspension was then inoculated on Mueller Hinton media using the streaking method. Wells (diameter 6mm) were created on the media in which 50µl of the sample (brown and pink peels extracts, nanoparticles synthesized from brown and pink extracts, silver nitrate) were added using a pipette. The controls used were Vancomycin (vancocip 500) and chloramphenicol (mediphenicol). The plates were incubated at 37 ℃ for 24 hours after which the zone of inhibition was measured [26]. The test was done in triplicates and the average results were calculated.

The enhancement/reduction of the crude extracts was compared to their respective nanoparticles. The activity of each nanoparticle synthesized was then compared to silver nitrate as well as the commercial test drugs. The activity of these variables was compared between the resistant and non-resistant *E. coli* and *S. aureus* strains. The level of enhancement/reduction of antimicrobial activity was calculated as follows where X and Y represent the variables being compared:

$$\frac{Average\ diameter\ of\ ZOI\ (mm)\ of\ X}{Average\ diameter\ of\ ZOI\ (mm) of\ Y}$$

3. Results and Discussion

3.1 Preparation of potato peel extract

The dry weight of the potato peels was determined to be 13.1% and 13.6 % for brown russet and red bliss potatoes. Potato peels had a high amount of water content which explains the reduction in weight of the peels after drying [27].

3.2 Phytochemical characterization

Major phytochemical compounds in plants such as flavonoid, saponin, phenol hydroquinone, alkaloid, sterol, tannin, and reducing sugar have polar properties and can be extracted by water, methanol, and ethanol [28]. The presence of flavonoids, phenols and tannins was confirmed as shown in Table 1. The presence of phenols was detected by the formation of a dark, green-black colour, while the formation of yellow-orange colour with the addition of alkali drops indicated the presence of flavonoids [21]. A yellow crystalline precipitate formation indicated the presence of alkaloids [22].

Table 1: Phytochemical testing of red bliss and brown russet potato peels aqueous extract.

	Phenol test	**Flavonoids test**	**Alkaloids test**
Russet brown peels	+ 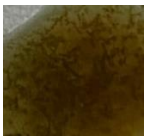	+ 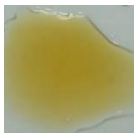	+ 
Red bliss peels	+ 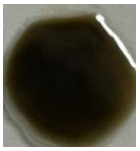	+ 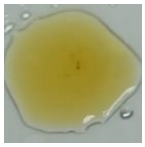	+ 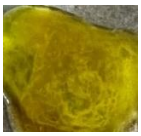

Both potato peel varieties showed positive results for phenols, flavonoids, and alkaloids. The intensity of colour was similar for flavonoids and alkaloids however, red bliss had an intense green-black colour as compared to russet brown for phenols. Numerous phytochemicals have been identified as agents responsible for nanoparticle synthesis such as flavonoids, polyphenols, proteins, polysaccharides, alkaloids, and alcoholic compounds [29]. The major phytochemical constituents of potato peel extract are polyphenols, flavonoids, and alkaloids such as solanine. Potato peels comprise up to 10 times more polyphenols than the tuber itself [27]. The phenolic acids present in potato peels include chlorogenic acids, gallic acid, protocatechuic acid, and caffeic acid [30].

3.3 AgNP synthesis Potato peel extract concentration optimization

Upon reacting the silver nitrate solution with three concentrations (0.05g/5ml, 0.1g/5ml, and 0.2g/ml) of the potato peel extract in water, and evaluating peak formation using UV-Vis spectrophotometer, the concentration of 0.05g/5ml resulted in the formation of a prominent peak within the range of 400-450nm in both varieties. Higher concentrations of extract did not produce any peaks except for brown russet with a concentration of 0.1g/5ml which resulted in a less intense peak at 415nm. A higher concentration of silver nitrate compared to the reducing agent, in this case, the potato peel extract increases the collisions of silver with the phytochemicals

causing agglomeration of silver nitrate and causing it to be undetected during UV-Vis analysis [23].

Time (min)	0	5	15
Russet Brown			
Red Bliss			

Figure 1: Change in colour of silver nitrate solution over time upon addition of potato peels aqueous extract

Both the potato peel varieties exhibited colour change from colourless silver nitrate solution to dark brown upon addition of the potato peel extract as shown in figure 1. The brown potato peels resulted in a dark brown colour within 5 minutes of the reaction while the pink potato peels took 15 minutes to form a dark brown colour, however, colour change was noticeable within 5 minutes of the reaction. A strong reductant results in a faster reaction rate [31]. The colour change indicated the formation of silver nanoparticles as a result of silver ion reduction. As the concentration of silver nanoparticles increases, the intensity of colour increases [32]. The phytochemicals present in biological materials are responsible for the synthesis of silver nanoparticles as they have reducing and stabilizing properties and can act as capping agents [31].

Scanning of the samples in UV-Vis spectrophotometer exhibited a peak within 400-450nm which indicated the presence of silver nanoparticles (Figure 2). The optimum peak for brown russet potato was 435nm while the optimum peak for red bliss potato was 430nm. The crude extracts and 1mM silver nitrate did not exhibit any peak in the same region, therefore confirming that no silver nanoparticles were present prior to biogenic synthesis.

Adjustment of pH from acidic to basic is important since low pH results in the formation of larger nanoparticles. A higher pH results in the reduction of the nanoparticle size. When pH increases, the concentration of positive ions H^+ reduces, and the concentration of OH^- ions increases which results in a higher negative charge which favours the reaction with Ag^+ ions. Nanoparticles are not formed above the optimum pH as agglomeration is favored [33]. pH plays an important role in controlling both the shape and the size of nanoparticles [32] . Temperature above normal room temperature was chosen i.e., 70°C. At a higher than room temperature, kinetic energy increases which results in a faster reaction rate, and more silver ions are consumed due to greater bombardment of molecules. This also results in smaller sized nanoparticles as there is less scope for growth [34].

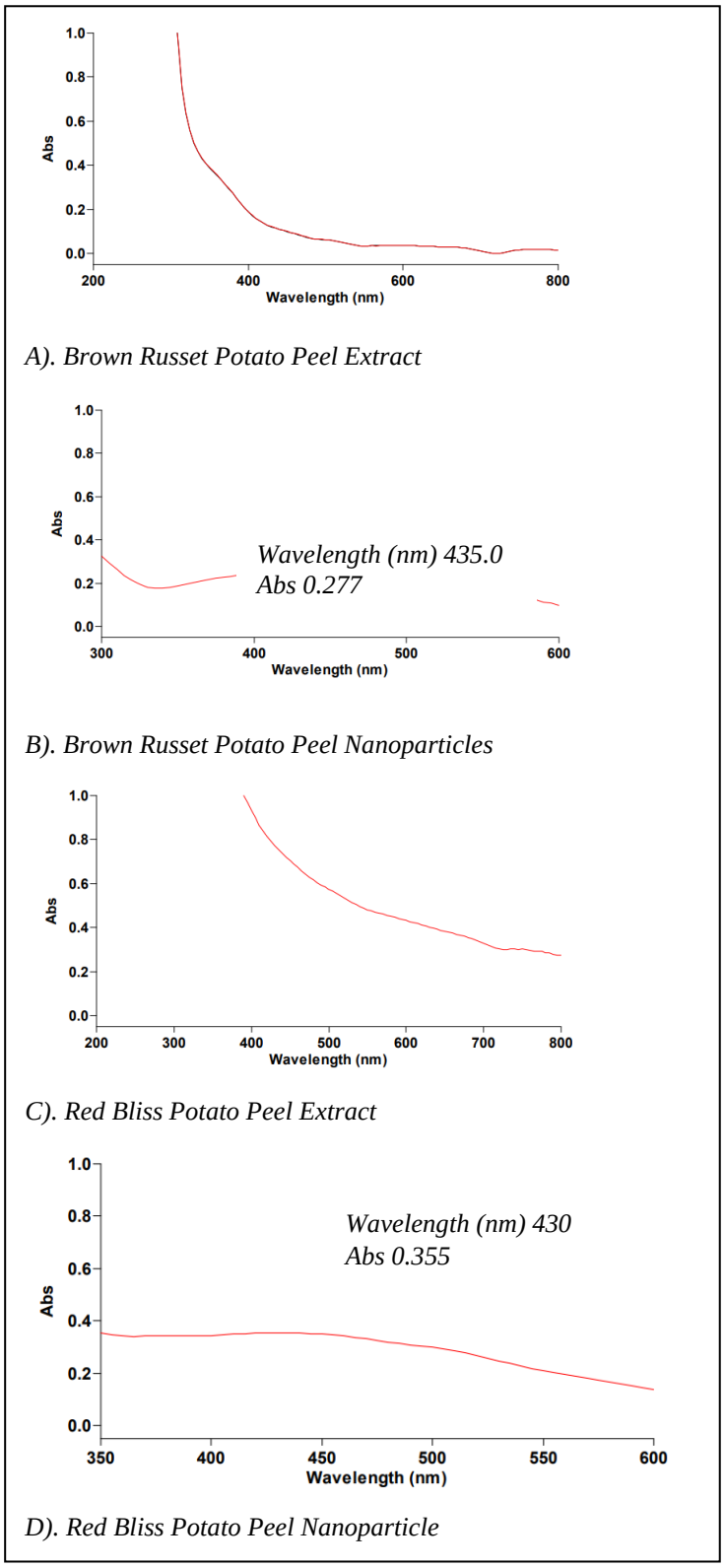

Figure 2: Uv-Vis spectrophotometry analysis of crude extract of Brown Russet and Red bliss peels aqueous extract and their respective nanoparticle

3.4 Dynamic light scattering and zeta potential

DLS results and zeta potential results for both potato peel nanoparticles have been reported as shown in table 2 below. Zeta potential measurements were carried out for both brown russet and red bliss potatoes to predict potential agglomeration and stability of colloidal particles while DLS was carried out for size analysis.

Table 2: DLS and zeta potential of brown russet and red bliss NP

Potato peel variety	Average diameter nm	Polydis persity index	Zeta potential mV
Brown russet NP	391.5 ± 13.55	0.421 ± 0.076	-25.6 ± 1.01
Red bliss NP	203.0 ± 3.770	0.320 ± 0.063	-32.7 ± 5.03

The ideal size should be between 1-100nm. However, dynamic light scattering-particle size analysis determined the size of the brown russet NP to be 391.5nm which was much higher than the 203nm particles size determined for the red bliss NP. The particle size of the AgNPs synthesized from both brown russet and red bliss was higher than the average nanoparticle size of between 1 to 100nm. This indicates agglomeration of the nanoparticles with time took place. This was similar to results observed previously where agglomeration with time was observed for nanoparticles [35]. Synthesis parameters also affect the nanoparticle size. A higher concentration of silver nitrate increases the collisions of silver, as the capping agent relative to biogenic synthesized silver nanoparticles are inadequate. The silver nanoparticles tend to agglomerate and increase in size [23].

The polydispersity index of both samples has a high value which indicates that polydisperse particles are present. This is attributed to the similar mechanism of agglomeration mentioned above. For both samples, there were nanoparticles present within the ideal 1-100nm range while majority exceed 100nm as shows in figure 3a and 3c. High zeta potential is indicative of higher stability of the colloidal particles [23]. The red bliss NP have higher stability than the brown russet NP. This means that the red bliss sample is stable and can maintain its particle size of 203.0 ± 3.770nm as it has a more negative zeta potential of -32.7 ± 5.03mV compared to that of brown russet sample -25.6 ± 1.01Mv (figure 3 b and d).

The negative charge is attributed to bioactive compounds which may be adsorbed on the surface of the silver nanoparticles [36] . The zeta potential of nanoparticles directly affects their antimicrobial activity as one of the mechanisms of action of silver nanoparticles involves electrostatic adhesion with the cell membrane [31].

3.5 FTIR analysis

FTIR analysis was carried out for both the crude extracts and their respective nanoparticles between 4000-500cm^{-1} as shown in figure 4 below. The FTIR of the crude extracts revealed numerous peaks indicating the presence of phytochemicals such as polyphenols, alkaloids, and flavonoids [29]. The FTIR spectra for the brown russet and red bliss peels are non-superimposable indicating variation in the phytochemicals present in both varieties with some common bands. The FTIR spectra comparison of the extract and AgNP allows the determination of the compounds responsible for the reduction and capping of AgNP. Upon synthesis of nanoparticles, alteration to peaks were visible in FTIR spectra with prominent peaks forming in both the nanoparticle varieties indicating that bio-reduction had taken place.

The bands present both the FTIR of the crude extracts and respective nanoparticles in the high-frequency region around 3781cm^{-1} to lower frequencies is due to the hydrogen-bonded O-H groups. The bands present between 1625–1440cm^{-1} are attributed to the C=C aromatic ring stretching and conjugated diketone and ketoester groups. The bands at lower frequencies between 1000-1050cm^{-1} represent C-O stretching corresponding to the presence of carboxylic acids, alcohols, esters, and ethers [37].

Upon the formation of nanoparticles, numerous shifts in peaks are observed with the formation of new peaks indicating active functional group utilization for nanoparticle synthesis. A new peak at 2076.96cm^{-1} was observed in both nanoparticles' FTIR corresponding to the C-N stretching vibration. A peak present only in the brown russet NP at 1349.96cm^{-1} corresponds to the NO_2 stretch of nitro compounds. There is a shift of bands corresponding to hydroxyl and carbonyl groups indicating utilization of phytochemicals present in the peels in the capping of silver nanoparticles [23].

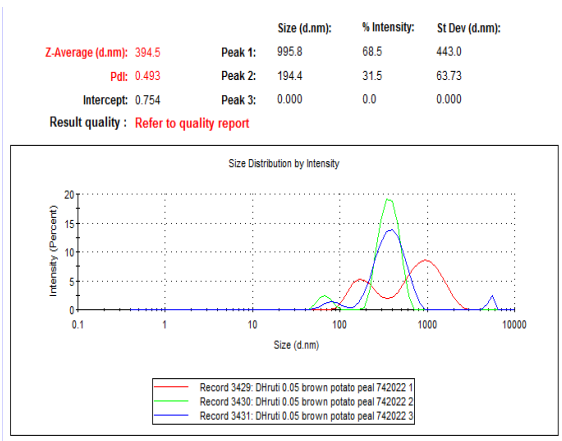

a) Russet brown nanoparticle size

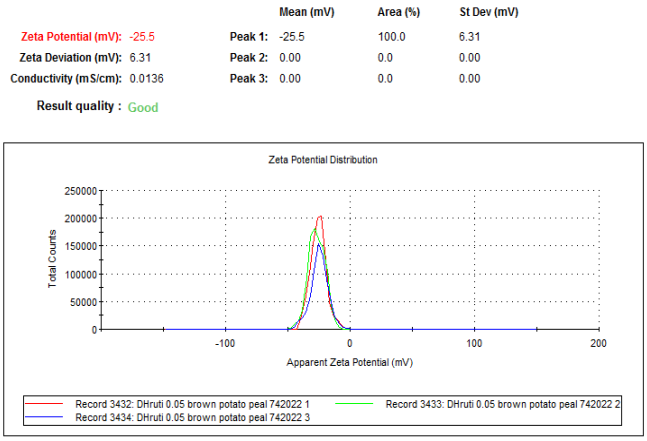

b). Russet brown nanoparticle zeta potential

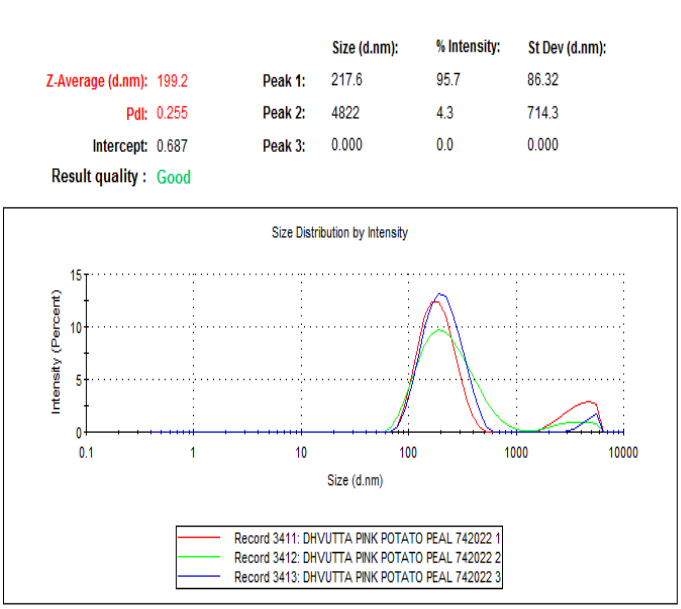

c) Red bliss nanoparticle size analysis

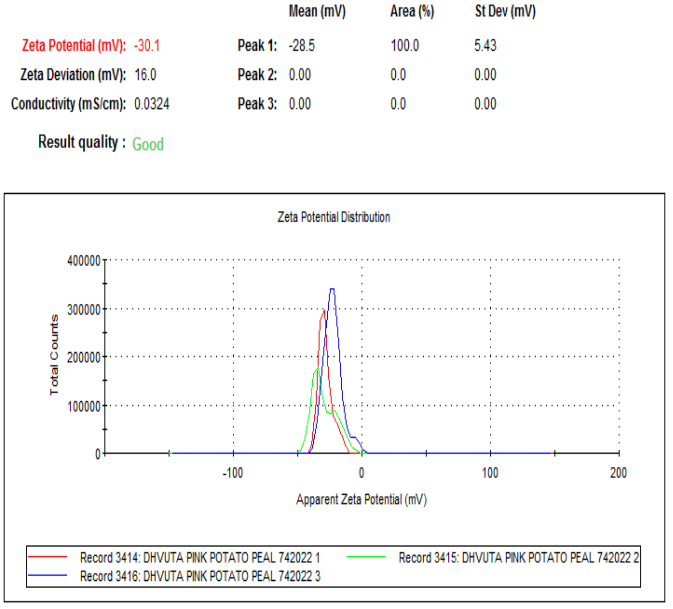

d) Red bliss nanoparticle zeta potential analysis

Figure 3*: Size and zeta potential analysis of the nanoparticles*

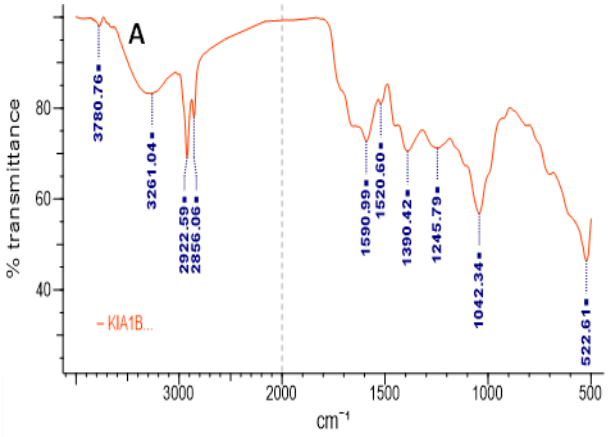

A: Russet brown potato peel aqueous extract

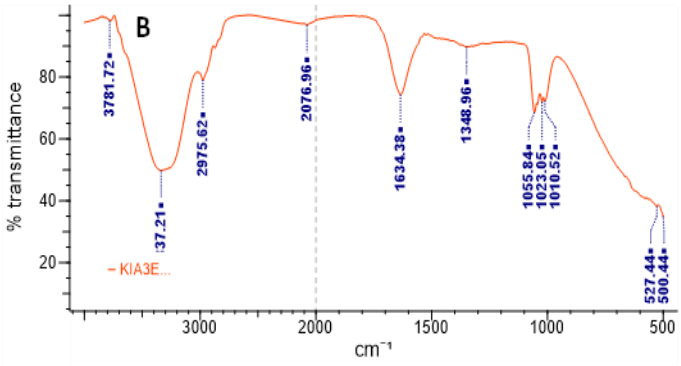

B: Russet brown potato peel nanoparticles

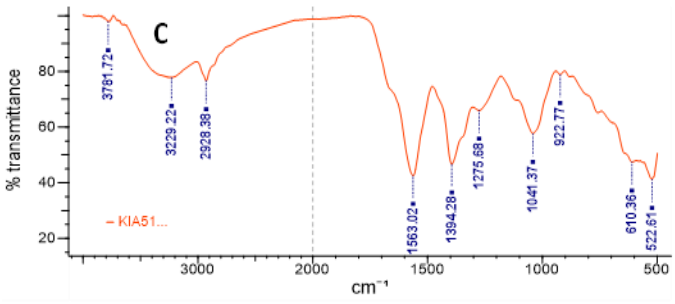

C: Red bliss potato peel aqueous extract

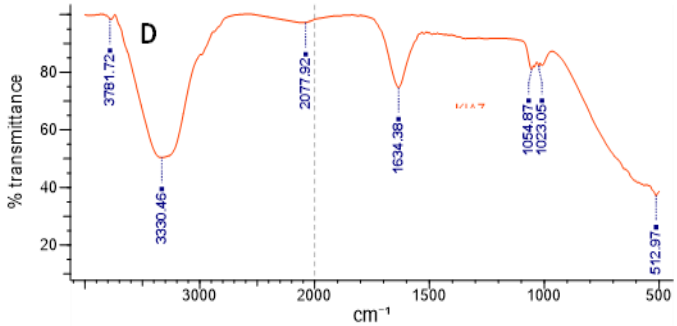

D: Red bliss potato peel nanoparticles

Figure 4: FTIR spectra of Russet brown and Red bliss potato peels aqueous extracts and synthesized nanoparticles between 4000-500cm^{-1}

3.6 Antimicrobial sensitivity test

The antimicrobial activity of the synthesized nanoparticles was tested on *S. aureus*, *E. coli*, and their multi-drug resistant strains using the disc diffusion technique and the hallow diameters determined as shown in figure 5.

No zones of inhibition were seen with the potato peels extracts which indicate that they did not have any antimicrobial activity. However, potato peels have been shown to exhibit antibacterial properties which are attributed to the fatty acids and lipids which may not have been present in the ethanol extract [27]. In addition, the antibacterial activity of plant extracts depends on concentration, with very low concentrations exhibiting no antibacterial activity [38]. The average zone of inhibition for the synthesized nanoparticles from russet brown peels was 9.3 ± 0.6 mm and 7.3 ± 0.6mm for multi-drug resistant *E. coli* and *E. coli* respectively. The zone of inhibition for the nanoparticles synthesized from red bliss potato was 1.3 times enhanced at 11.7 ± 0.6mm and 1.1 times enhanced at 8.3 ± 0.6mm for multi-drug resistant E. coli and *E. coli* respectively. Therefore, the red bliss peel nanoparticles exhibited better antibacterial activity against *E. coli* than russet brown peel nanoparticles.

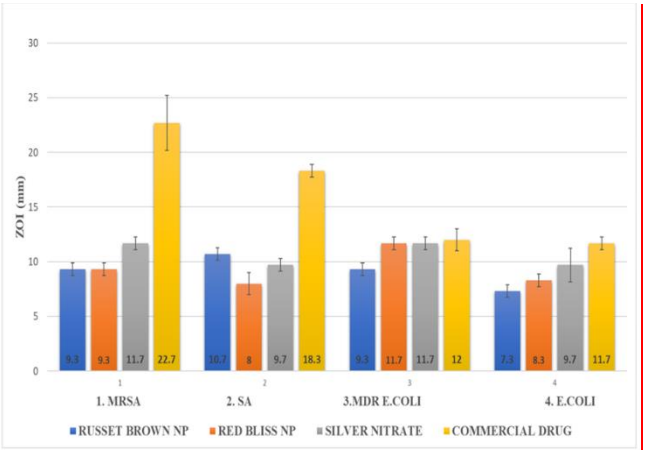

Figure 5: Average zone of Inhibition by the different potato peels extracts against *S. aureus*, *E. coli*, and their multidrug resistance stains *S. aureus* (MRSA) and *E. coli*

The average zone of inhibition for the synthesized nanoparticles from russet brown peels was 9.3 ± 0.6mm and 10.7 ± 0.6mm for MRSA and SA respectively. The zone of inhibition for the nanoparticles synthesized from red bliss potato was the equivalent at 9.3 ± 0.6mm and 0.7 times diminished at 8.0 ± 1.0mm for multi-drug resistant MRSA and SA respectively (figure 5). Therefore, the russet brown peel nanoparticles exhibited better antibacterial activity against *S. aureus* than red bliss nanoparticles. This was observed in another study where better activity was observed against gram-positive than gram-negative bacteria possibly due to the protective lipopolysaccharide layer present in gram-negative bacteria [39].

Biogenic synthesized nanoparticles from the potato peels showed activity against both gram-positive and gram-negative species (figure 5). However, red bliss potato peel nanoparticles showed better activity against E. coli than S. aureus. The average ZOI for MRSA was diminished by 0.8% at 9.3 ± 0.6mm than that for multi-drug resistant E. coli at 11.7 ± 0.6mm. This was similar to results obtained in previous studies that depicted enhanced antibacterial activity of biogenic nanoparticles on gram-negative bacteria as compared to gram-positive bacteria [32]. The zone of inhibitions is different for both types of bacteria. This can be attributed to the structure of the cell wall. Gram-positive bacteria have a thicker peptidoglycan layer than gram-negative bacteria. However, gram-negative bacteria have lipopolysaccharides in addition to the thin peptidoglycan layer which impacts the mechanism of action of silver nanoparticles [40].

Silver nanoparticles have multiple mechanisms of antimicrobial action. The cell membrane of bacterial cells contributes to the formation of silver ions when silver nanoparticles are exposed to oxygen or hydrogen peroxide and undergo oxidative dissolution. These silver ions are hypothesized to induce bacterial destruction by binding negatively charged proteins, DNA, and respiratory enzymes with a thiol group. The silver ion prevents DNA replication by forming dimers with thiol groups present in DNA. The thiol groups are also present in proteins and cell membranes which are denatured by the formation of S-Ag bonds. Silver nanoparticles also result in direct cell membrane damage by attachment and penetration of the cell membrane [23]. These multiple mechanisms could be responsible for similar antibacterial activity observed in both the MDR and Non-MDR strains. Silver nanoparticles can also form bonds with aromatic hydrocarbons and form polyelectrolyte complexes. These complexes prevent the transport of solutes which are necessary for the survival of the bacteria [32].

Silver nitrate also had an antibacterial activity which is attributed to the presence of silver ions. The average zone of inhibition for silver nitrate for the resistant and non-resistant strains was 11.7 ± 0.6 mm and 9.7 ± 0.6 mm respectively for both S. aureus and E. coli (fig 5). The peel nanoparticles exhibited varied antibacterial activity with russet brown having 1.1 times enhanced activity against SA than silver nitrate while multi-drug resistant E. coli had equivalent activity as silver nitrate. The lower antibacterial activity of nanoparticles for the other species compared to silver nitrate can be attributed to silver ions. Silver ions have shown to have better antimicrobial activity than AgNP. This is depicted even at low Ag ion concentrations [41].

The conventional antibiotics have 2 times enhanced antimicrobial activity against S. aureus strains as that for the nanoparticles as depicted in figure 5. However, they are more prone to antimicrobial resistance than silver nanoparticles as the latter elicit their action using multiple simultaneous steps [23]. The nanoparticles synthesized using the red bliss peels exhibited similar activity with 1

times enhancement to the commercially available drug; tetracycline for MDR *E. coli* at 11.7 ± 0.6mm and 12 ± 1.0 mm respectively. This shows the potential of the biogenic route of nanoparticle synthesis in combating antimicrobial resistance as compared to conventional antibiotics.

4. Conclusion

Nanoparticles were synthesized using peels of both potato varieties with a peak between 400-450nm in a UV-Vis spectrophotometer. The particle size of the synthesized AgNPs was however higher than the average nanoparticle size indicating a possible agglomeration of the nanoparticles. FTIR analysis confirmed the reduction of silver ions by ethanol-soluble phytochemicals present in potato peels. Both potato peels varieties exhibited antibacterial activity against both the gram-negative and positive species including the drug resistance species.

Russet brown peel nanoparticles had a better antimicrobial activity by 1.3 times enhanced activity on multidrug resistance E. coli than E. coli and less antibacterial activity against MRSA by 0.9 compared to S. aureus. On the contrary, red bliss NP had better antibacterial activity by 1.25 against the multidrug resistance *E. coli* strains. Compared to conventional methods, biogenic synthesis using natural products is pivotal in providing economical nanoparticles by eliminating the use of costly reagents which pose an additional threat to the environment. More studies are however needed to minimize the agglomeration of the AgNPs.

Acknowledgments

The authors wish to acknowledge Ms. Lucy Wambui, botanist and taxonomist for plant identification as well as Mr. Eugene Otoo for support in preparation of aqueous extract.

DECLARATIONS

Conflicts of interest

The authors declare no conflict of interest.

Ethical statement

Ethical approval to conduct the research was obtained from the USIU-Africa institutional review board. The application approval number is USIU-A/IRB/394/2021. All biocontainment measures were considered while using the microorganisms.

Contribution of each authors

The listed authors have significantly contributed to the manuscript as follows:

Kerai, D.N: Participated in inception of the project idea, performed laboratory experiments and drafted the manuscript**.**

Mbatia, B.N: Participated in inception of the project idea, guided laboratory experiments on extraction of phytochemicals and antimicrobial assays, reviewed the manuscript.

Noah, N.M: Guided laboratory experiment on nanoparticles synthesis and characterization, reviewed the manuscript**.**

References

[1] Gajdács M, Urbán E, Stájer A, Baráth Z. Antimicrobial resistance in the context of the sustainable development goals: A brief review. Eur J Investig Heal Psychol Educ 2021;11:71–82. https://doi.org/10.3390/ejihpe11010006.

[2] Dadgostar P. Antimicrobial Resistance: Implications and Costs 2019. https://doi.org/10.2147/IDR.S234610.

[3] Wang L, Hu C, Shao L. The antimicrobial activity of nanoparticles: Present situation and prospects for the future. Int J Nanomedicine 2017;12:1227–49. https://doi.org/10.2147/IJN.S121956.

[4] Turner NA, Sharma-Kuinkel BK, Maskarinec SA, et al. Methicillin-resistant Staphylococcus aureus: an overview of basic and clinical research. Nat Rev Microbiol 2019;17:203. https://doi.org/10.1038/s41579-018-0147-4.

[5] Burrus V, Poulin-Laprade D, Canada A-F, et al. Citation: A Clinical Extensively-Drug Resistant (XDR) Escherichia coli and Role of Its β-Lactamase Genes 2020. https://doi.org/10.3389/fmicb.2020.590357.

[6] Gavamukulya Y, Maina EN, Meroka AM, et al. Green Synthesis and Characterization of Highly Stable Silver Nanoparticles from Ethanolic Extracts of Fruits of Annona muricata. J Inorg Organomet Polym Mater 2020;30:1231–42. https://doi.org/10.1007/S10904-019-01262-5.

[7] Lee N-Y, Ko W-C, Hsueh P-R. Nanoparticles in the Treatment of Infections Caused by Multidrug-Resistant Organisms. Front Pharmacol 2019;0:1153. https://doi.org/10.3389/FPHAR.2019.01153.

[8] Slavin YN, Asnis J, Häfeli UO, Bach H. Metal nanoparticles: understanding the mechanisms behind antibacterial activity. J Nanobiotechnology 2017 151 2017;15:1–20. https://doi.org/10.1186/S12951-017-0308-Z.

[9] Almatroudi A. Silver nanoparticles: synthesis, characterisation and biomedical applications. Open Life Sci 2020;15:819–39. https://doi.org/10.1515/BIOL-2020-0094.

[10] Anees Ahmad S, Sachi Das S, Khatoon A, et al. Bactericidal activity of silver nanoparticles: A mechanistic review. Mater Sci Energy Technol 2020;3:756–69. https://doi.org/10.1016/J.MSET.2020.09.002.
[11] Singh J, Dutta T, Kim K-H, Rawat M, Samddar P, Kumar P. "Green" synthesis of metals and their oxide nanoparticles: applications for environmental remediation. J Nanobiotechnol 2018;16:84. https://doi.org/10.1186/s12951-018-0408-4.
[12] Marslin G, Siram K, Maqbool Q, et al. Secondary Metabolites in the Green Synthesis of Metallic Nanoparticles. Mater 2018, Vol 11, Page 940 2018;11:940. https://doi.org/10.3390/MA11060940.
[13] USAID-KAVES POTATO VALUE CHAIN ANALYSIS 2015:5.
[14] Mäder J, Rawel H, Kroh LW. Composition of Phenolic Compounds and Glycoalkaloids α-Solanine and α-Chaconine during Commercial Potato Processing. J Agric Food Chem 2009;57:6292–7. https://doi.org/10.1021/JF901066K.
[15] Sinha N, Dua D. Evaluation of antioxidant and antimicrobial properties of potato (Solanum tuberosum) peels. Indian J Agric Biochem 2016;29:23–7. https://doi.org/10.5958/0974-4479.2016.00004.6.
[16] Anjum R, R AS, Karthikeyan M, et al. Solanum tuberosum L: Botanical, Phytochemical, Pharmacological and Nutritional Significance. Int J Phytomedicine 2018;10:115–24. https://doi.org/10.5138/09750185.2256.
[17] Valcarcel J, Reilly K, Gaffney M, O'Brien NM. Antioxidant Activity, Total Phenolic and Total Flavonoid Content in Sixty Varieties of Potato (Solanum tuberosum L.) Grown in Ireland. Potato Res 2015 583 2015;58:221–44. https://doi.org/10.1007/S11540-015-9299-Z.
[18] Al-Weshahy A, Rao VA. Potato Peel as a Source of Important Phytochemical Antioxidant Nutraceuticals and Their Role in Human Health - A Review. Phytochem as Nutraceuticals - Glob Approaches to Their Role Nutr Heal 2012. https://doi.org/10.5772/30459.
[19] María del Carmen Robles-Ramírez, Ricardo Monterrubio-López, Rosalva Mora-Escobedo. Evaluation of extracts from potato and tomato wastes as natural antioxidant additives 2016. https://www.alanrevista.org/ediciones/2016/1/art-8/ (accessed November 2, 2021).
[20] Chandra Joshi N, Chhabra J, Kaur K, Thakur A. Potato tuber extract based synthesis, characterisation and antibacterial activity of silver nanoparticles 2020.
[21] Yadav R, Agarwala M. Phytochemical analysis of some medicinal plants. J Phytol 2011;3:10–4.
[22] Shaikh JR, Patil M. Qualitative tests for preliminary phytochemical screening: An overview. Int J Chem Stud 2020;8:603–8. https://doi.org/10.22271/chemi.2020.v8.i2i.8834.
[23] Wibowo A, Tajalla GUN, Marsudi MA, et al. Green synthesis of silver nanoparticles using extract of cilembu sweet potatoes (Ipomoea batatas l var. rancing) as potential filler for 3d printed electroactive and anti-infection scaffolds. Molecules 2021;26. https://doi.org/10.3390/molecules26072042.
[24] Shah M, Fawcett D, Sharma S, Tripathy SK, Poinern GEJ, Elbahri M. Green Synthesis of Metallic Nanoparticles via Biological Entities 2015. https://doi.org/10.3390/ma8115377.
[25] Syed ZHN, Uroo K, Muhammad IA, et al. Combined efficacy of biologically synthesized silver nanoparticles and different antibiotics against multidrug-resistant bacteria 2013. https://doi.org/10.2147/IJN.S49284.
[26] Das G, Patra JK, Basavegowda N, Vishnuprasad CN, Shin H-S. Comparative study on antidiabetic, cytotoxicity, antioxidant and antibacterial properties of biosynthesized silver nanoparticles using outer peels of two varieties of Ipomoea batatas (L.) Lam . Int J Nanomedicine 2019;14:4741–54. https://doi.org/10.2147/IJN.S210517.
[27] Javed A, Ahmad A, Tahir A, et al. Potato peel waste-its nutraceutical, industrial and biotechnological applacations. AIMS Agric Food 2019 3807 2019;4:807–23. https://doi.org/10.3934/AGRFOOD.2019.3.807.
[28] Widyawati PS, Budianta TDW, Kusuma FA, Wijaya EL. Difference of solvent polarity to phytochemical content and antioxidant activity of Pluchea indicia Less leaves extracts 2014.
[29] Iravani S, Korbekandi H, Mirmohammadi S V, Zolfaghari B. Synthesis of silver nanoparticles: chemical, physical and biological methods. vol. 9. 2014.
[30] Samarin AM, Poorazarang H, Hematyar N, Elhamirad A. Phenolics in Potato Peels: Extraction and Utilization as Natural Antioxidants. World Appl Sci J 2012;18:191–5. https://doi.org/10.5829/idosi.wasj.2012.18.02.1057.

[31] Roy A, Bulut O, Some S, Mandal AK, Yilmaz MD. Green synthesis of silver nanoparticles: biomolecule-nanoparticle organizations targeting antimicrobial activity. RSC Adv 2019;9:2673–702. https://doi.org/10.1039/C8RA08982E.

[32] Ahmadi O, Jafarizadeh-Malmiri H, Jodeiri N. Eco-friendly microwave-enhanced green synthesis of silver nanoparticles using Aloe vera leaf extract and their physico-chemical and antibacterial studies. Green Process Synth 2018;7:231–40. https://doi.org/10.1515/GPS-2017-0039/MACHINEREADABLECITATION/RIS.

[33] Ndikau M, Noah NM, Andala DM, Masika E. Green Synthesis and Characterization of Silver Nanoparticles Using Citrullus lanatus Fruit Rind Extract. Int J Anal Chem 2017;2017. https://doi.org/10.1155/2017/8108504.

[34] Verma A, Mehata MS. Controllable synthesis of silver nanoparticles using Neem leaves and their antimicrobial activity. J Radiat Res Appl Sci 2016;9:109–15. https://doi.org/10.1016/J.JRRAS.2015.11.001.

[35] Tomaszewska E, Soliwoda K, Kadziola K, et al. Detection limits of DLS and UV-Vis spectroscopy in characterization of polydisperse nanoparticles colloids. J Nanomater 2013;2013. https://doi.org/10.1155/2013/313081.

[36] Yusuf SNAM, Mood CNAC, Ahmad NH, Sandai D, Lee CK, Lim V. Optimization of biogenic synthesis of silver nanoparticles from flavonoid-rich Clinacanthus nutans leaf and stem aqueous extracts. R Soc Open Sci 2020;7:200065. https://doi.org/10.1098/RSOS.200065.

[37] Bouhadjra K, Lemlikchi W, Ferhati A, Mignard S. Enhancing removal efficiency of anionic dye (Cibacron blue) using waste potato peels powder. Sci Rep 2021;11. https://doi.org/10.1038/S41598-020-79069-5.

[38] Debalke D, Birhan M, Kinubeh A, Yayeh M. Assessments of Antibacterial Effects of Aqueous-Ethanolic Extracts of Sida rhombifolia's Aerial Part. Sci World J 2018;2018. https://doi.org/10.1155/2018/8429809.

[39] Cavassin ED, de Figueiredo LFP, Otoch JP, et al. Comparison of methods to detect the in vitro activity of silver nanoparticles (AgNP) against multidrug resistant bacteria. J Nanobiotechnology 2015;13:64. https://doi.org/10.1186/S12951-015-0120-6.

[40] Loo YY, Rukayadi Y, Nor-Khaizura MAR, et al. In Vitro antimicrobial activity of green synthesized silver nanoparticles against selected Gram-negative foodborne pathogens. Front Microbiol 2018;9:1555. https://doi.org/10.3389/FMICB.2018.01555/BIBTEX.

[41] Kędziora A, Speruda M, Krzyżewska E, Rybka J, Łukowiak A, Bugla-Płoskońska G. Similarities and Differences between Silver Ions and Silver in Nanoforms as Antibacterial Agents. Int J Mol Sci 2018, Vol 19, Page 444 2018;19:444. https://doi.org/10.3390/IJMS19020444.

Recommended Citation

Kerai D., Betty M., & Naumih N. Synthesis of silver nanoparticles using Solanum tuberosum peels' extract and their activity against multi drug resistant bacteria. *Alger. j. biosciences*. 2023, 04(02):123-132.